Proceedings of XIX International Scientific Conference "New Technologies and Achievements in Metallurgy, Material Engineering, Production Engineering and Physics", Częstochowa, Poland, June 7–8, 2018

Structural, Magnetic and Mechanical Properties of Dual-Phase $Ni_{50}Mn_{25}Ga_{20}Gd_5$ Magnetic Shape Memory Alloy

A. Łaszcz*, M. Hasiak and J. Kaleta

Wrocław University of Science and Technology, Faculty of Mechanical Engineering, Department of Mechanics, Materials Science and Engineering, M. Smoluchowskiego 25, 50-370 Wrocław, Poland

The microstructure, magnetic and mechanical properties of the annealed at 1430 K $Ni_{50}Mn_{25}Ga_{20}Gd_5$ (at.%) magnetic shape memory alloy were studied. The $Ni_{50}Mn_{25}Ga_{20}Gd_5$ ingot was prepared in a bulk form by arc-melting method. Scanning electron microscopy supported by atomic force microscopy investigations confirmed a dual-phase microstructure of the studied alloy characterized by Gd-poor and Gd-rich phases. Temperature dependence of magnetic magnetization $M(T)$ measured at high ($\mu_0 H = 2$ T) and low ($\mu_0 H = 0.25$ T) value of external magnetic fields revealed that the fabricated material undergoes reversible martensitic transition close to the room temperature. The Curie temperature for the investigated material calculated from the $M(T)$ curve measured in zero-field cooled mode is 377 K. Mechanical properties of the $Ni_{50}Mn_{25}Ga_{20}Gd_5$ alloy investigated by the means of a series of nanoindentation tests allowed to separate hardness for the Gd-poor (435 HV) and Gd-rich (562 HV) phase.

DOI: 10.12693/APhysPolA.135.301

PACS/topics: 75.50.Cc, 75.60.Ej, 81.30.Kf, 81.70.Bt, 62.20.de, 62.20.fg

1. Introduction

Magnetic shape memory alloys (MSMA) based on Ni–Mn–Ga composition are one of the most interesting group of modern smart materials [1–4]. These alloys have gained increasing attention due to their multifunctional properties, such as magnetic shape memory effect [1], superelasticity [2], magnetoresistance [3] or giant magnetocaloric effect [4]. All abovementioned properties of MSMA stem from their complex magnetostructural behaviour. Moreover, Ni–Mn–Ga alloys undergo the first-order reversible martensitic transformation from high-temperature austenite to low-temperature martensite phase. One of the method to change both magnetic and mechanical properties of the NiMnGa-based materials (together with their phase transition temperatures) is partial substitution of Ni, Mn, or Ga atoms by a forth doping element [5–7]. It was previously reported by certain researchers that Gd could be a beneficial alloying element, as it increases strength and ductility of material and shifts martensitic transformation temperatures to room temperature regime [8, 9]. In this paper, the microstructure, magnetic, and mechanical properties of the novel $Ni_{50}Mn_{25}Ga_{20}Gd_5$ MSMA are studied.

2. Experimental procedure

NiMnGa-based MSMA with a nominal composition of $Ni_{50}Mn_{25}Ga_{20}Gd_5$ (at.%) was prepared by arc-melting method in a form of button-shape ingot under a protective argon atmosphere. In order to obtain homogeneity, the ingot was remelted several times. In the next step the sample was sealed in a vacuumed quartz tube and annealed at 1430 K for 3 h. The microstructure and topography of the prepared material were analysed by scanning electron microscope (JSM-5800LV, JEOL), and atomic force microscope (XE-100, Park System) in contact mode. Thermomagnetic $M(T)$ curves in zero-field cooled (ZFC) and field cooled (FC) modes in the temperature range from 50 K to 400 K and external magnetic field of 0.25 T and 2 T were measured by VersaLab System (Quantum Design). DC hysteresis loops for selected temperatures were recorded with the help of the same system in a magnetic field up to 2 T. In order to reduce the demagnetization field the investigated sample for DC magnetic measurements was in a form of needle. The magnetizing field was applied along the needle edge. To investigate mechanical properties of the studied alloy, prepared sample was subjected to a series of nanoindentation tests carried out on Nanoindentation Tester (NHT2, CSM Instruments). For the purpose of these measurements surface of the sample were mapped with 100 indents using maximum load of 20 mN. Collected data were then evaluated with respect to Oliver-Pharr protocol [10, 11]. The statistical analysis allowed to separate hardness (HV) and elastic modulus (E_{IT}) for each individual phase in the material.

3. Results and discussion

Figure 1 depicts SEM images of the $Ni_{50}Mn_{25}Ga_{20}Gd_5$ sample obtained from both secondary electron (SE) and backscatter electron (BSE) detector. It is well seen, especially in the BSE image (Fig. 1b), that the $Ni_{50}Mn_{25}Ga_{20}Gd_5$ alloy is characterized by dual-phase microstructure. The high contrast between dark matrix

*corresponding author; e-mail: amadeusz.laszcz@pwr.edu.pl

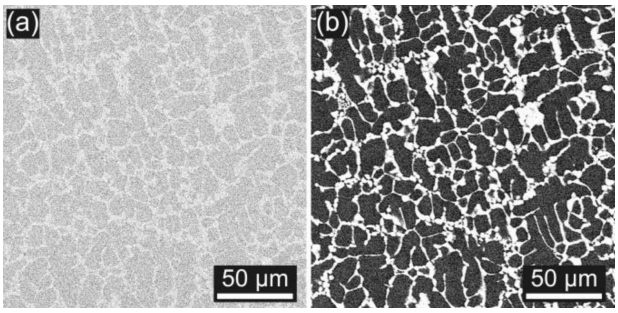

Fig. 1. (a) Secondary electron (SE) and (b) backscatter electron (BSE) images of the same area observed for the $Ni_{50}Mn_{25}Ga_{20}Gd_5$ alloy.

phase and bright phase along the matrix grain boundaries suggests the notable difference of Gd concentration in these two phases, due to the high atomic number of Gd compares to Ni, Mn, or Ga element. Considering that fact, bright phase was described as Gd-rich phase, while dark phase, by analogy, as Gd-poor phase.

Microstructural investigation performed by AFM measurements in contact mode for the same region of the $Ni_{50}Mn_{25}Ga_{20}Gd_5$ alloy is presented as 2D and 3D images in Fig. 2. The highest difference between the measured points on the image is only 12 nm, but it is clearly seen that surface morphology of the sample reflects to the same dual-phase microstructure, as it was seen on the SEM images (Fig. 1).

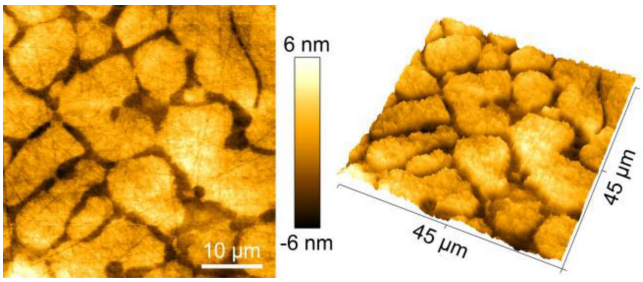

Fig. 2. 2D (left) and 3D (right) AFM images of the $Ni_{50}Mn_{25}Ga_{20}Gd_5$ alloy scanned in contact mode.

In order to get strong understanding of the magnetic properties of the $Ni_{50}Mn_{25}Ga_{20}Gd_5$ alloy, the temperature dependences of magnetization in zero-field cooled and field cooled modes at low ($\mu_0 H = 0.25$ T) and high ($\mu_0 H = 2$ T) value of external magnetic field were measured. Recorded thermomagnetic curves, shown in Fig. 3, indicate that the investigated material undergoes the reversible martensitic transition. This transformation occurs mainly in the Gd-poor phase, whose chemical composition is close to the Ni_2MnGa phase. On the $M(T)$ characteristic the martensitic transformation is observed as an abrupt change in magnetization. For the external magnetic field of 0.25 T, sudden drop on $M(T)$ curve on the FC branch corresponds to the martensitic transformation from austenite ($M_s = 281$ K) to martensite

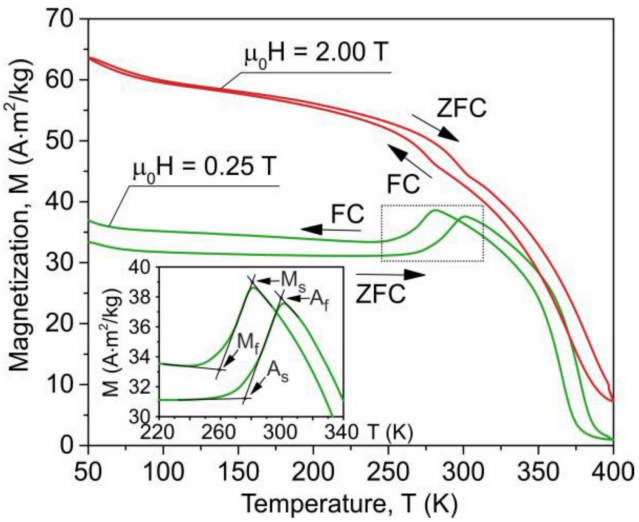

Fig. 3. Thermomagnetic $M(T)$ curves for the $Ni_{50}Mn_{25}Ga_{20}Gd_5$ alloy recorded in ZFC and FC modes at the external magnetic field of 0.25 T and 2 T. The inset shows martensitic transition region of the curve measured at 0.25 T.

TABLE I

Temperatures of structural and magnetic transitions for the $Ni_{50}Mn_{25}Ga_{20}Gd_5$ alloy (M_s/M_f — martensite transition start/finish temperature, A_s/A_f — austenite transition start/finish temperature, T_C^H/T_C^C — the Curie temperature during heating/cooling process determined from the minimum position of the dM/dT curve)

M_s [K]	M_f [K]	A_s [K]	A_f [K]	T_c^H [K]	T_c^C [K]
281	259	276	300	377	366

($M_f = 259$ K) phase. Consequently, rapid increase in magnetization on the ZFC branch corresponds to the reversible martensitic (austenitic) transformation from martensite ($A_s = 276$ K) to austenite ($A_f = 300$ K) phase. All temperatures for both structural and magnetic transitions are summarized in Table I. Smaller value of magnetization of about 35 A m^2/kg for the martensite phase and almost flat characteristic of the ZFC and FC $M(T, \mu_0 H = 0.25$ T) curve after martensitic transformation suggests that martensite phase has a larger magnetostructural anisotropy than austenite phase. On the other hand, $M(T, \mu_0 H = 2$ T) recorded for the $Ni_{50}Mn_{25}Ga_{20}Gd_5$ alloy decreases constantly during the heating process. Additionally, only a slight kink on the discussed $M(T)$ curve in the vicinity of martensitic transition temperature is visible. Comparable $M(T)$ magnetic characteristics observed for the $Ni_{50}Mn_{25}Ga_{20}Gd_5$ alloy were also reported for others NiMnGa-based alloys [12–14]. Presented phenomenon implies that at high values of external magnetic field magnetostructural anisotropy has not significant influence on magnetization behaviour.

Figure 4 presents DC hysteresis loops of the $Ni_{50}Mn_{25}Ga_{20}Gd_5$ alloy measured at indicated temperatures. The loops recorded at 50 K, 150 K and 200 K

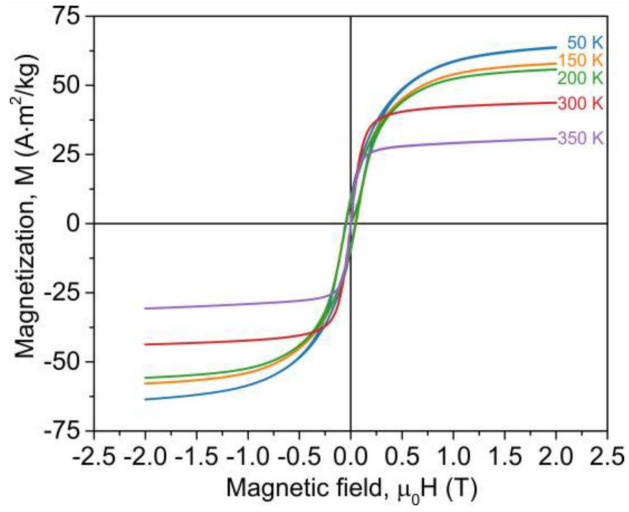

Fig. 4. DC hysteresis loops $M(H)$ for the $Ni_{50}Mn_{25}Ga_{20}Gd_5$ alloy measured at the indicated temperatures from 50 K to 350 K.

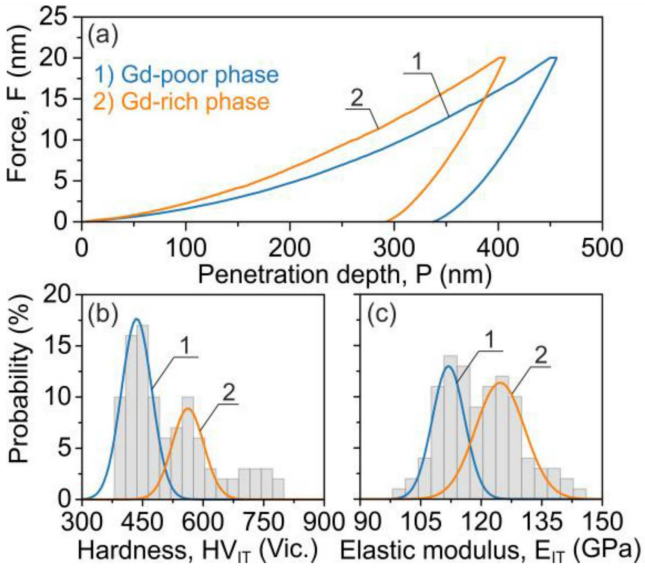

Fig. 5. (a) Examples of load versus intender displacement curves for the Gd-poor and Gd-rich phase in the $Ni_{50}Mn_{25}Ga_{20}Gd_5$ alloy together with distributions of (b) hardness and (c) elastic modulus for these phases.

correspond to the martensite phase, while the loops obtained at 300 K and 350 K describe magnetic behaviour of the austenite phase. From this figure, it is well seen that the austenite phase is notably more softer and easily saturated than the martensite phase.

The mechanical properties of the dual-phase $Ni_{50}Mn_{25}Ga_{20}Gd_5$ alloy were studied at the room temperature by the means of a series of nanoindentation tests. The use of 100 indents grid combined with optical analysis allowed to separate the mechanical properties for the Gd-poor and Gd-rich phases. Figure 5a depicts the example of load versus indenter displacement curves for two existing phase. It is well known that instrumented measurements of load–displacement curves provide not only information about plastic deformation of investigated materials, but also about their elastic behaviour during unloading. Figure 5b and c presents the distributions of the Vickers hardness and elastic modulus of the studied sample. Presented results show that Gd has substantial influence on mechanical properties of the Ni–Mn–Ga system, as hardness of the Gd-rich and Gd-poor phase equals to 562 HV and 435 HV, respectively. The same tendency is also displayed for the elastic modulus, which equals 125 GPa for the Gd-rich phase and 112 GPa for the Gd-poor phase (Fig. 5c).

4. Conclusions

The microstructure, magnetic, and mechanical properties of the Gd-doped $Ni_{50}Mn_{25}Ga_{20}Gd_5$ MSMA were studied in the presented work. Fabricated material reveals dual phase microstructure with a clear difference between Gd-rich and Gd-poor phases. Temperature dependence of magnetization of the studied alloy were used to estimate temperatures of both structural and magnetic transformation. It was found that temperatures of reversible martensitic transition are close to the room temperature, whereas the Curie points occur at about 377 K. The nanoindentation studies shown that addition of Gd to Ni–Mn–Ga composition improves mechanical properties of Ni–Mn–Ga system.

References

[1] O. Heczko, *Mater. Sci. Tech. Lond.* **30**, 1559 (2014).
[2] M.F. Qian, X.X. Zhang, C. Witherspoon, J.F. Sun, P. Müllner, *J. Alloys Comp.* **577S**, S296 (2013).
[3] D. Pal, K. Mandal1, O. Gutfleisch, *J. Appl. Phys.* **107**, 09B103 (2010).
[4] A. Planes, L. Manosa, M. Acet, *J. Phys. Condens. Matter.* **21**, 233201 (2009).
[5] C.L. Tan, G.F. Dong, L. Gao, J.H. Sui, Z.Y. Gao, W. Cai, *J. Alloys Comp.* **538**, 1 (2012).
[6] I. Glavatskyy, N. Glavatska, O. Söderberg, S.P. Hannula, J.U. Hoffmann, *Scr. Mater.* **54**, 1891 (2006).
[7] S. Fabbrici, G. Porcari, F. Cugini, M. Solzi, J. Kamarad, Z. Arnold, R. Cabassi, F. Albertini, *Entropy* **16**, 2204 (2014).
[8] X. Zhang, J. Sui, X. Zheng, Z. Yang, W. Cai, *Mater. Sci. Eng. A* **597**, 178 (2014).
[9] W. Cai, L. Gao, Z.Y. Gao, *J. Mater. Sci.* **42**, 9216 (2007).
[10] W.C. Oliver, G.M. Pharr, *J. Mater. Res.* **7**, 1564 (1992).
[11] W.C. Oliver, G.M. Pharr, *J. Mater. Res.* **19**, 3 (2004).
[12] L. Straka, O. Heczko, *J. Appl. Phys.* **93**, 8636 (2003).
[13] F.Q. Zhua, F.Y. Yang, C.L. Chien, L. Ritchie, G. Xiao, G.H. Wu, *J. Magn. Magn. Mater.* **288**, 79 (2005).
[14] T. Sakon, H. Nagashio, K. Sasaki, S. Susuga, D. Numakura, M. Abe, K. Endo, S. Yamashita, H. Nojiri, T. Kanomata, *J. Phys. Chem. Solids* **74**, 158 (2013).